

Optoelectrical anisotropy in Graphene oxide supported polythiophene thin films fabricated by floating film transfer

Rajiv K. Pandey,¹ Atul S. M. Tripathi,² Shyam S. Pandey² and Rajiv Prakash¹

¹School of Materials Science and Technology, Indian Institute of Technology (Banaras Hindu University), Varanasi-221005, India.

²Graduate School of Life Science and System Engineering, Kyushu Institute of Technology, 2-4 Hibikino, Wakamatsu, Kitakyushu 808-0196, Japan

Corresponding Author Email: rprakash.mst@iitbhu.ac.in

Abstract

A facile method for the fabrication of highly oriented hybrid thin films of conjugated polymer (CP) with graphene oxide (GO) as 2D nano-filler over the high surface tension liquid substrate by floating film transfer is being reported. Formation of the self-assembled oriented hybrid thin film has been validated using multiple characterization techniques. Hybrid thin films thus prepared have been used for the fabrication of organic field effect transistors (OFETs) followed by investigation of anisotropic charge carrier transport. OFETs made with hybrid films oriented in channel direction exhibited the superior device performance with >6 fold augmentation in field effect mobility (μ) and one order improvement in on/off ratio as compared to that of devices based on pristine CP. However, pristine polymer shows 2.2 fold enhancement in mobility and one order augmentation in on/off ratio in parallel orientation as compared to the corresponding perpendicularly oriented films. Thus, our study has elucidated a path to obtain oriented, aligned, and self - assembled hybrid films for further improvement in the device performance aiming towards the applications in organic electronics.

Keywords: Phase transferred GO; Self-Assembly; Hybrid nanomaterials; Floating film transfer; anisotropic charge transport; OFET

1. Introduction

The opportunity for the exploration of conducting polymer (CP) thin films and its 2D polymer nano-hybrid have recently attracted huge attention owing to their extraordinary performance and exceptional functionality [1-2]. Apart from this, only few thin film technologies have taken off from the laboratory level to industry with certain limitations [3-5]. It is important here to mention that charge carrier mobility is highly dependent upon the polymer backbone alignment and orientation [6-8], which can be controlled via directed self-assembly during thin film processing. In addition to film forming technique, nature of CP, its molecular weight and nano materials to make nano-hybrid etc. are some of the major factors that govern the quality of polymer in thin films [9-11]. By amending the processing conditions, such as self-organization of CPs over 2D nanosheets [12], size of crystalline domains as well as length of conducting path can be substantially increased. It is now well-known that there is facile carrier transport along the polymer chains owing their inherent one-dimensionality and improved carrier hopping in π - π stacking direction, which is highly essential for planar device like organic field transistors (OFETs). We would like to introduce a highly facile fabrication of CP/graphene oxide (GO) nano-hybrid thin films over viscous liquid substrate named as floating film transfer method (FTM). This method is not only able to resolve the existing challenges of solution based thin film fabrication techniques but also provide the molecular alignment by self-assembly during film fabrication. Novelty of this work lies in the implementation of two methods, where first one is the phase transfer of 2D nanosheets without using any surfactants and ultra-sonication in order to prevent the modification of 2D nanosheets [13]. Secondly, use of high surface tension and viscous liquid substrate for the preparation of polymer nano-hybrid thin films at air-liquid interface by FTM. It also eliminates post thermal annealing process for the promoted molecular alignment offering potentiality for the large area flexible electronics devices [14-15]. FTM is very similar to Langmuir-Schaefer technique [16] in terms

of use of the air-liquid interface but do not need application of external pressure for molecular alignment. On the other hand, viscosity of liquid substrate acts like dragging force during spreading floating film leading to molecular alignment.

Here, we have used the GO as 2D material for the preparation of its nanohybrid with poly (3,3'-didodecyl-quaterthiophene) (PQT) as organic semiconductor, which provide two extremely different dimensions. One-dimensional thin oriented polymeric chains of PQT and the lateral macroscopic GO with large surface area ranging up to several hundreds of micrometres [17-19]. It is noteworthy that work function of these nano-materials also lies within the HOMO and LUMO of the PQT, which creates a charge transfer interface between polymer/2D nanomaterial without any energy barrier between CP and graphene [20]. In this manuscript, we have synthesized the GO via improved hummer's method and obtained 4 layer thick nanosheets via phase transfer method using ultrasonication for formation CP decorated GO nanohybrid solution. Nature of the FTM processed thin films of PQT/GO were investigated by morphological, structural, fast Fourier transform (FFT) and polarized electronic absorption spectral characterizations. The obtained results were also compared with the pristine floating film of CP. Finally, OFETs were fabricated using the nanohybrid oriented thin films as active semiconductor in bottom gate top contact (BGTC) device architecture for anisotropic electrical characterization and extraction of device parameters.

2. Experimental

2.1. Synthesis of GO via phase transfer and decoration of GO nano sheets with PQT polymer

In order to synthesize the GO nanosheets from graphite powder, improved Hummers method was employed as per our earlier publication [21]. As obtained GO was used for phase transfer from aqueous dispersion to chloroform. Schematic representation of phase transfer and fabrication of polymer

decorated GO nanosheets has been shown in Fig. 1. Details about the preparation of semiconducting PQT has been given in our earlier publication [22]. In brief, rigorous sonication was used to form a homogeneous dispersion of GO in water (1 mg/ml). Further, CHCl_3 was added in an aqueous dispersion of GO (equal volume), which produce a clear interface (bi-phase) of CHCl_3 and water due to immiscibility. CHCl_3 remain in the bottom due to its higher specific gravity and aqueous dispersion remains at the top. GO was transferred to CHCl_3 via 2 hr. sonication. Original picture of phase transferred GO in CHCl_3 have been shown in Fig S1.

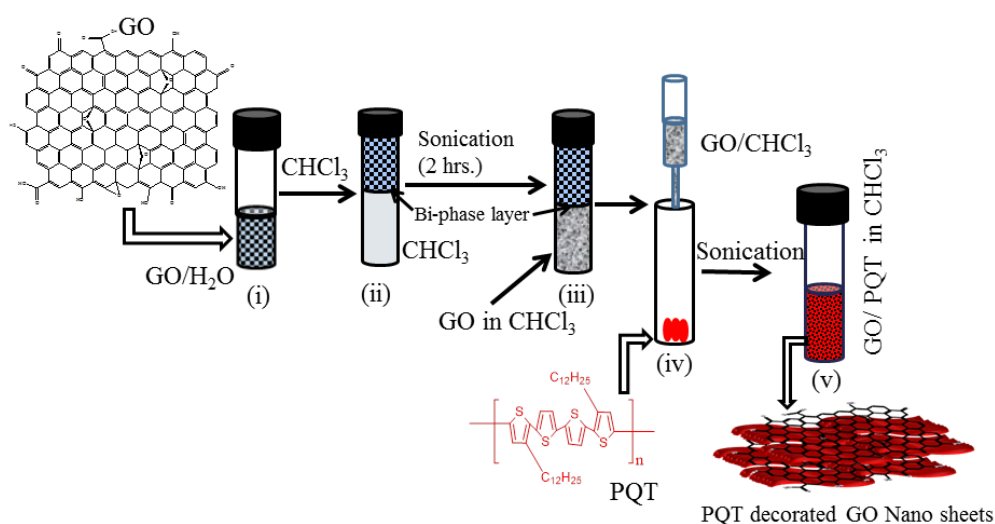


Fig. 1. Schematics for relocation of GO from water dispersion to CHCl_3 and formation of PQT decorated GO nanosheets.

A 200 μl of GO/CHCl_3 dispersion was used to prepare 10 mg/ml (w/v) solution of PQT in a sealed vial. In order to decorate the GO nanosheets with polymer chains, it was kept under sonication for two hrs. to acquire PQT decorated GO hybrid solution.

2.2. Synthesis of PQT decorated/ GO nanohybrid thin film.

A drop (15 μl) of PQT/GO in chloroform was dropped liquid substrate composed of ethylene glycol (EG) and glycerol (GL) in 3:1 ratio at room temperature leading to fabrication of thin floating film. The

development of hybrid film has been discussed in detail in the results and discussion section [23]. Further, as prepared film over EG/GL was transferred on to desired substrates by stamping and dried at 60°C before various characterization and study of charge transport along and across the polymer alignment after fabricating the OFETs in the BGTC device configuration. Atomic force microscope (AFM) was used to measure the thickness of PQT/GO hybrid film and found to be $\sim 15 \pm 1$ nm (Fig S4).

2.3. Characterization tools

High resolution transmission electron microscopy (HR-TEM), scanning transmission electron microscopy (STEM) and selected area electron diffraction (SAED) and fast Fourier transform (FFT) was acquired via Tecnai G² (New Zealand). Electronic absorption spectra were obtained via JASCO V-570 spectrophotometer equipped with a Glan Thomson polarizer to see the effect of 2D nanosheets on dichroic ratio (DR) of polymer films at macroscopic level. To probe the optical anisotropy in the fabricated thin films, optical dichroic ratio (DR) was calculated using the formula, $DR = \frac{A_{\parallel}}{A_{\perp}}$, (where A_{\parallel} and A_{\perp} are maximum absorption along and orthogonal to the orientation direction). Further, grazing incidence X-ray diffractometry (GIXD) was conducted for the structural analysis as well as orientation, which was attached with in-plane diffractometer (Rigaku, Japan). GIXD was recorded at 0.2° incident angle for all samples. Raman spectrum was recorded using a SPR 300 Raman spectrometer attached with 532 nm laser. Atomic force microscopy (AFM) was scanned via NT-MDT, Russia, under semi-contact mode. Lastly, charge transport properties and device parameters fabricated OFETs was probed using Keithley source meter (Model- 2612A).

3. Results and discussion

3.1. Characterizations of phase transferred GO nanosheets

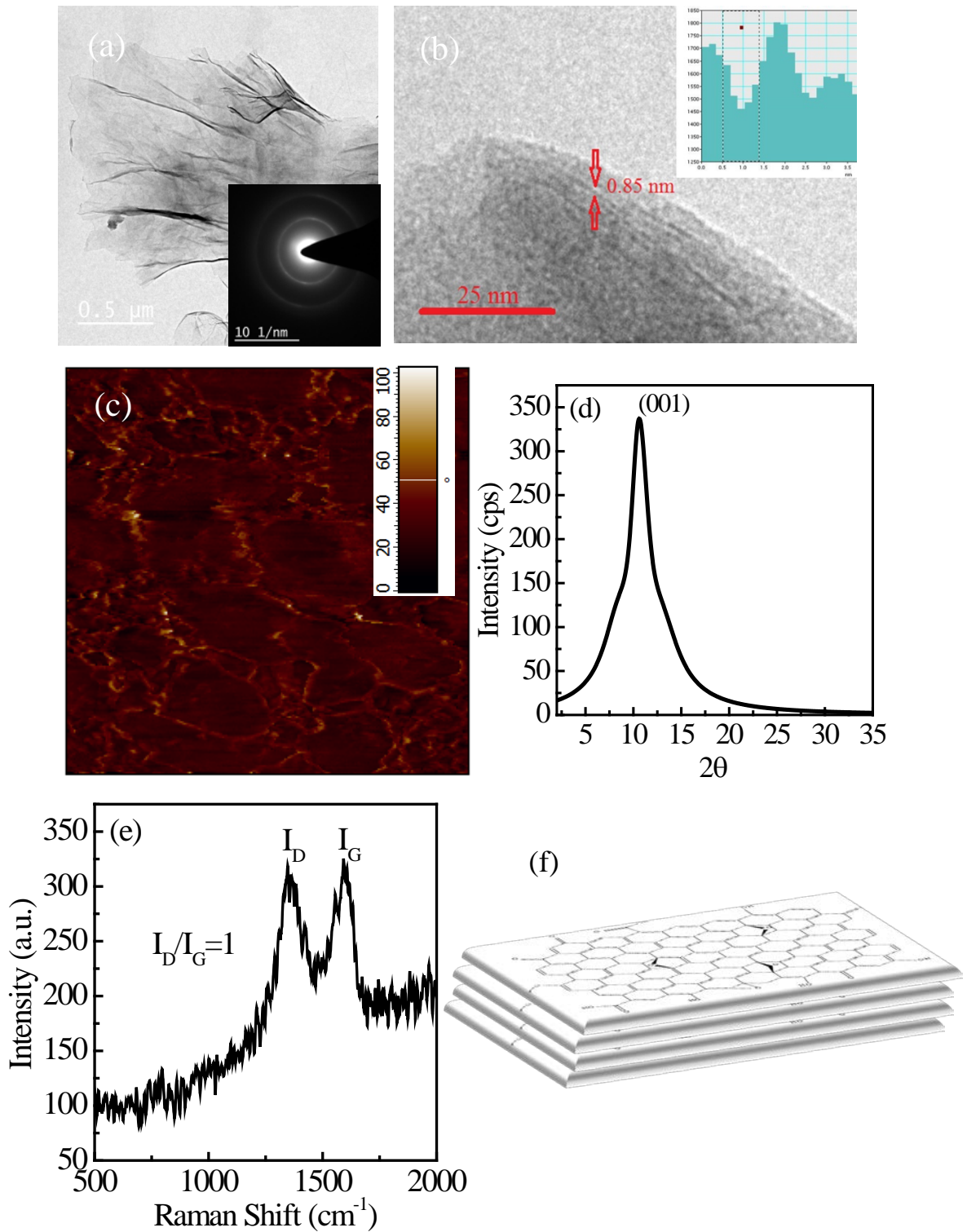


Fig. 2 (a). TEM image of GO nanosheet. Inset shows the SAED pattern with (001) plane. (b) HR-TEM image showing (001) plane with 0.85 nm interlayer distance. Inset shows the interlayer distance measured during HR-TEM measurement. (c) AFM phase image of GO nanosheets. (d) GIXD of GO (e) Raman spectrum (f) Schematics for multilayer GO nano sheets with functionalized edges.

Prior to use of phase transferred GO dispersion for PQT/GO nanohybrid thin film formation, TEM, SAED, Raman spectroscopy and XRD were used to confirm and investigate the different properties such as morphology, structure and calculation of 2D nanosheets layers. The surface morphology of GO obtained by HR-TEM reveals the size, vacillating from hundreds of nanometre to micron level, which twists and folds at several places (Fig 1(a)). These twists and folds at several places arise due to incorporation of functional group over nanosheets carrying sp^3 hybridized carbon atoms during the oxidation process. Further, in order to analyse the structure of GO nanosheets, SAED measurement was conducted of same region as shown TEM image. SAED analysis (inset of Fig. 1(a)) confirms only (001) plane, which have been confirmed further using XRD discussed later. HR-TEM analysis at the edge of same sample reveals the formation of GO layer with thickness of ~ 4 nm and inter layer spacing of 0.85 nm which correspond to 4 to 5 layers of GO after phase transfer as shown in Fig 2(b). In order to validate the obtained result for GO by TEM and HR-TEM, AFM was conducted in two mode viz. height and phase in order to investigate the thickness and phase analysis. AFM height mode analysis (Fig. S2) demonstrates the average height of GO ~ 4 -5 nm, which confirms the thickness of GO in obtained HR-TEM.

It is essential to mention here that we have measured phase image contemporarily, viz during the AFM height image measurement. Bellunato et. al has reported that the high chemical reactivity on the edge arises due to unsaturated p_z orbital and break of π conjugation, differ from the relative inertness of basal plane of graphene [24]. Phase analysis of GO via AFM shows $\sim 100^\circ$ change in phase angle at edges of GO sheets as compared to basal plane, which validates the presence of high density of functional group at edges. It is notable here that we have conducted the GIXD measurement

of same sample in order to predict the crystal structure, interlayer spacing, number of layers etc. as shown in Fig 2(d). GIXD of GO demonstrates single peak at 10.65° and can be assigned as (001) plane. The relation $d_{hkl} \sin\theta = n\lambda$, (where d_{hkl} is interlayer spacing and λ is the wavelength of X-ray used in XRD) was employed to calculate the interlayer spacing of GO nanosheets and found to be 0.83 nm, which is very close to the value obtained from HR-TEM. We have employed the formula, $L_c = \frac{0.9\lambda}{\beta \cos\theta}$ (Scherrer's formula), to estimate the layers, where L_c is coherence length, and rest symbol have their usual meanings. This reveals the L_c of phase transferred GO around was ~ 3.4 nm with ~ 4 to 5 numbers of GO layers, which is similar to the number of layer obtained by HR-TEM and AFM height images. For comparison, we have also carried out XRD of as synthesised GO (Fig. S5), which reveals L_c of 6.2 nm and corresponds to 7 to 8 numbers of layers in sheets.

Figure 2(e) shows the Raman spectrum of GO nanosheets in the range of 500 to 2000 cm^{-1} , which demonstrates the two characteristics peak of GO at 1364 cm^{-1} and 1585 cm^{-1} , respectively. These two peaks can be attributed to disorder (D) and graphitic (G) band, respectively, where G is also known as the first-order Raman band and can be attributed to all C=C bonds of carbon. On the other hand, D band arises due to the presence of certain imperfections, incorporated during oxidation process of GO. It is worth to mention here that the ratio of I_G and I_D determine the quality of the nanosheets.. In our result, the I_D/I_G ratio was found to be 1. Raman spectrum was also recorded in the range 1500 - 3000 cm^{-1} for estimation of number of layers using I_G/I_{2D} ratio (Fig S6) of 4, which is very close to the result obtained from HR-TEM and GIXD.

3.2. Formation of self-assembled, aligned and oriented PQT thin films decorated GO nanohybrid

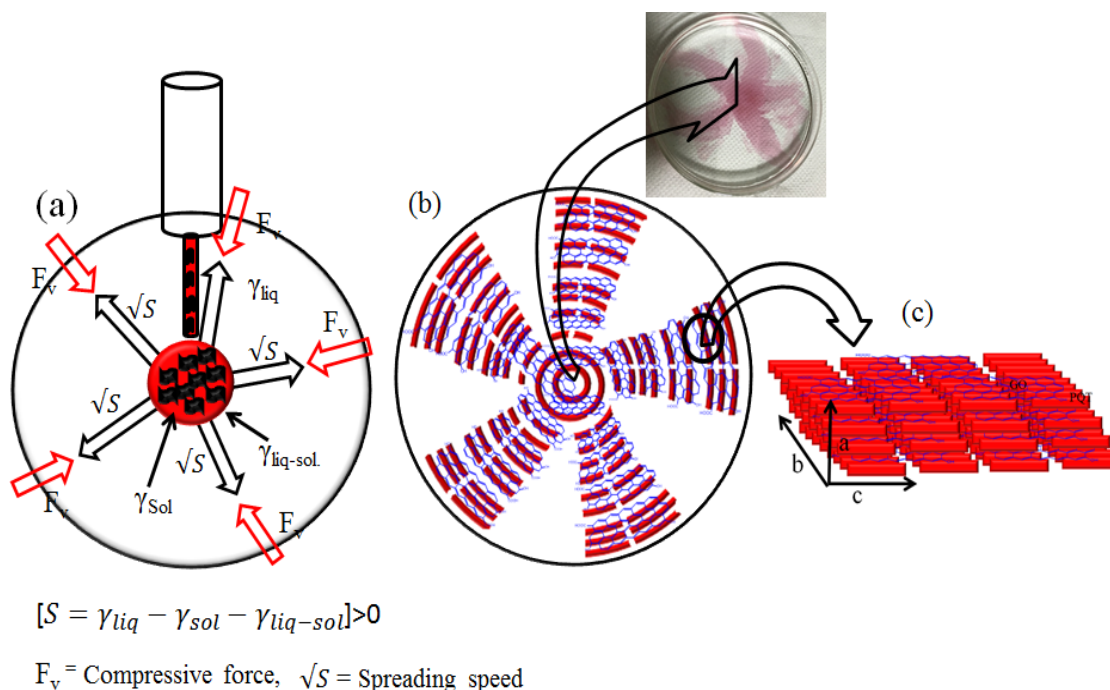


Fig. 3. Representation of the precise growth of CP/GO thin film on the surface of high surface tension liquid substrate accomplished by surface tension gradient and compressive force (a). Flow of hybrid solution on the liquid substrate depends on spreading coefficient S , which is directly related to equation $S = \gamma_{liq} - \gamma_{sol} - \gamma_{liq-sol}$, where γ_{liq} , γ_{sol} and $\gamma_{liq-sol}$ are surface tension of mobile liquid substrate, solution and mobile liquid-solution interfaces (b). Positive S results in a surficial flow of solution. However, viscous force (F_v) act as compressive force, results in formation of uniform compact, aligned and oriented nano-hybrid film in star shape. Inset shows the real picture of PQT/GO nanohybrid film floating over EG/GL liquid substrate. Schematic illustrations of formation of PQT decorated GO nanosheets with edge on oriented aligned polymer chains (c).

A small drop of PQT decorated GO in chloroform (CF) was dropped in the centre of a petri dish comprising of the mixture of EG/GL in the ratio of 3:1, where surface tension of each surface such as EG/GL-air, CF- air, and EG/GL-CF are assigned as γ_{liq} , γ_{sol} and $\gamma_{liq-sol}$, respectively as shown in Fig. 3(a). The local surface tension gradient causes the flow of low surface tension hybrid solution in CF along the EG/GL surface from low surface tension to higher surface tension [25-26]. The surface tension of CF, EG and GL was 27, 47 and 64 mN/m at room temperature resulting in to positive

spreading coefficient (+S), where $S = \gamma_{\text{liq}} - \gamma_{\text{sol}} - \gamma_{\text{liq-sol}}$. The proportion $S^{1/2}$, which is directly related to the mass transfer per unit time at EG/GL interface describes the spreading speed of the solution. Meanwhile, there is viscous force (F_v), which acts at interface of CF and EG/GL in inward direction [27-28] and is directly related to the spreading speed $S^{1/2}$ and poses a compressive force. Soeda et. al have used the compressive force using mechanical compression for formation of anisotropic film over ionic liquid at high temperature [29]. However, we have optimized and used viscosity as compressive force at room temperature. It is also noteworthy that two-factors viz. surface tension gradient causing the spreading of solution and viscosity induces the molecular alignment of PQT decorated GO nanosheet during the spreading of solution.

It is important to mention here that GO sheets are decorated with PQT polymer. GO bears macroscopic carbon network with terminal hydroxyl (-OH) groups and fraction of OH is very small as compared graphene moiety. Therefore, GO also spreads with polymer in spite of having -OH group at the edges and basal plane. We have used the chloroform as solvent for making PQT/GO solution, which is highly volatile. Therefore, CF evaporates very quickly (<1 sec) during spreading and the dried hybrid film remains floating over the liquid substrate after solvent evaporation a characteristic of FTM. Optimization of the FTM parameters such hydrophilic liquid substrate, viscosity, and evaporation rate of CHCl_3 at room temperature causes the development of star like, compressed, self- assembled, aligned and edge-on oriented polymer films as shown in Fig 3(b). Inset of Fig 3(b) shows the original picture of film, floating over EG/GL liquid-air interface. We transferred these floating films on to a desired solid substrate just by stamping and characterized using different techniques. In this article, we have later confirmed the development of crystalline, edge on oriented, aligned polymer thin film via different techniques as shown in Fig 3(c).

3.3. Morphological characterization

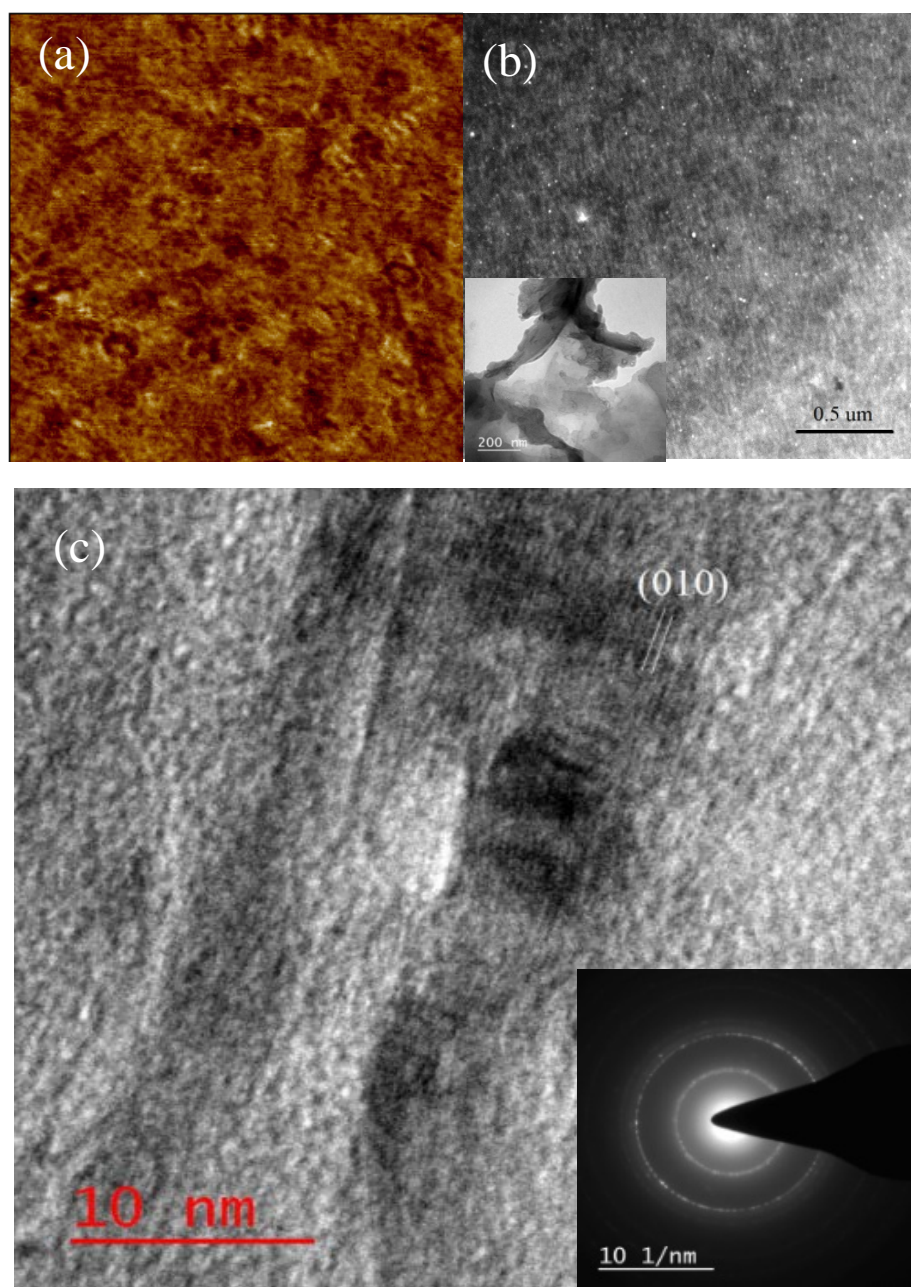


Fig. 4. (a) AFM image of PQT/GO hybrid floating film (scan area $3\mu\text{m} \times 3\mu\text{m}$) and (b) STEM micrograph of the PQT-GO hybrid floating film with oriented fibril of PQT. Inset displays the TEM image of PQT-GO hybrid film. (c) HR-TEM micrograph of PQT-GO hybrid floating film showing (010) plane. Inset displays the SAED pattern hybrid film.

In order to probe the alignment of polymer at microscopic level, we recorded the AFM image ($3\mu\text{m} \times 3\mu\text{m}$) as well as STEM image as shown in Fig. 4 (a, and b). However, the inset of Fig 4(b) shows the TEM image of same exhibiting the uniform distribution of GO in PQT polymer matrix with decoration of PQT nanostructures over GO sheets. Morphological characterization using AFM and STEM image of PQT/GO hybrid thin films demonstrate the aligned π - π stacked lamella with fibril like structure. Further, in order to investigate the alignment of polymer, HR-TEM image was recorded, which demonstrate the fringes of highly aligned and extended polymer chains with spacing 0.37 nm (Fig. 4(c)). This 0.37 nm inter planner spacing corresponds to π - π stacking and can be assigned as (010) plane only. This type of morphology has already been reported for crystalline; edge on oriented polythiophene by guided solidification [30]. Therefore, our hybrid film is highly edge-on oriented and crystalline due to presence of GO nanosheets and processing methodology, which has been further proved macroscopically using GIXD, FFT and polarized absorption spectra. Anisotropic nature of the polymer thin film fabricated by FTM, crystallinity and edge on orientation are desired features for fabricating the high performance planar devices like OFETs by placing the source-drain contacts in the orientation direction. The inset of Fig. 4(c) demonstrates the SAED pattern of a hybrid film. Hybrid floating film shows two type of plane as demonstrated in inset of Fig 4(c). One corresponds to (0k0) plane, which corresponds to PQT. However, (00l) plane resemble to GO. The presence of (0k0) plane reflects the formation of a crystalline domain of polymer. However, presence of (00l) plane confirms the polymer matrix with closely decorated PQT nanostructures. Thus, morphological characterization authenticates the formation of crystalline, highly oriented hybrid film with 0.37 nm of inter-planer spacing between π - π stacking.

3.4. Structural Analysis

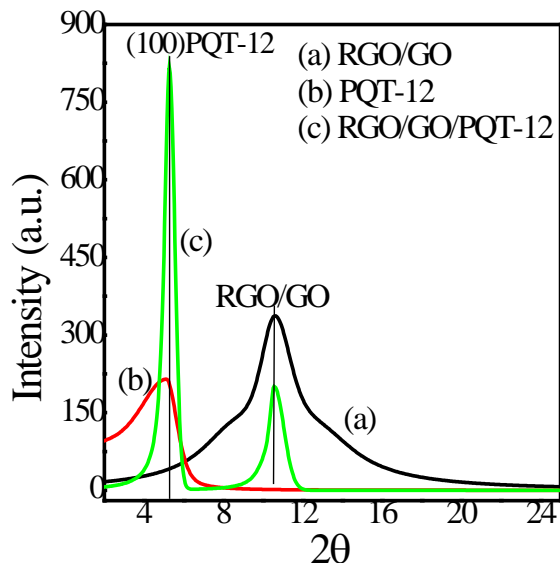


Fig. 5. GIXD of (a) GO film deposited after phase transfer, (b) pristine PQT and (c) PQT-GO hybrid floating film.

GIXD with fixed 0.2° grazing angle for GO nanosheets, PQT and PQT/GO films are shown in the Fig. 5. Further, GIXD investigation of pristine PQT shows a reflection corresponding to 100 plane at $2\theta = 4.90^\circ$, which arises only due to the side chain ordering. Further investigation of PQT/GO nano-hybrid film shows two peaks. The first peak appears at 5.06° with higher intensity and shifting towards higher 2θ angle, which correspond to (100) plane and the second peak appearing at a similar position of GO, which validates the formation of a PQT/GO nano hybrid film. It is observed that (100) peak of hybrid film shifted at higher 2θ angle as compared to that of pristine polymer and appear at 5.06° , which illustrate the better self-assembled crystalline film, in which nano-fibrils act as template. In order to probe the effect of 2D nanosheets on crystalline properties of the floating thin films quantitatively, we have calculated correlation length ' L_c ' of reflection peaks to approximate the mean crystallite size via the Scherrer equation. Although the Scherrer's relation is applied for calculation of crystallite

dimension but due to disordered nature of CP crystallites, it is difficult to calculate exactly crystallite dimension. Therefore, it is termed as coherence length L_c and is applied only for the comparison of crystallite sizes present in both of the samples [31]. The L_c of hybrid film was found to be ~ 4 fold higher as compare to the pristine polymer films. Thus, appearance of highly aligned lamella in AFM, STEM, only (010) plane in HR-TEM, and appearance of only (100) plane in GIXD discloses the highly edge on oriented PQT/GO hybrid film. This type of structure is highly essential, where charge transport occurs along the film plane.

3.5. Investigation of molecular alignment and optical anisotropy

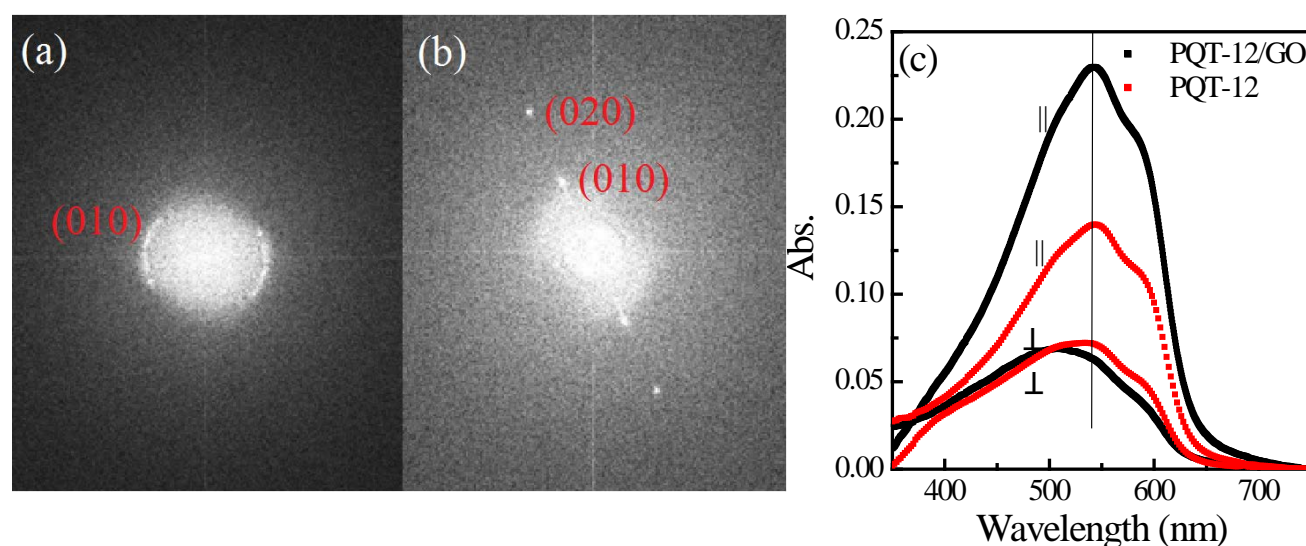


Fig. 6. Fast Fourier transform (FFT) of (a) pristine polymer film and (b) PQT/GO nano hybrid films. Polarised electronic absorption spectra of PQT-GO and pristine PQT (c) floating films \parallel and \perp to plane of polarization of light, respectively.

In order to investigate the local alignment of polymer chains, we conducted the Fast Fourier transform (FFT) TEM measurement of pristine PQT and hybrid PQT/GO films as shown in the Fig 6(a & b). It is noteworthy that FFT provides the information about diffraction pattern (reciprocal space) of the selected localized region in the high-resolution image and it can be associated with the SAED

patterns and hence alignment. The comparison of FFT of both films reveals the plausible differences such as hybrid film shows bright spot, lie in 2nd and 4th quadrant. However, there is no such scenario with pristine CP film. Pristine CP film shows broken circle as shown in Fig. 6 (a). The appearance of bright spot in hybrid film reveals the high alignment of polymer at microscopic level, which has confirmed earlier by HR-TEM image. Similar type of investigation was also reported by Biniek et. al for optically anisotropic films [32]. Although, HR-TEM image reveals the (0k0) planes, which validate the formation π - π stacked structure. Therefore, the spot correspond to (0k0) planes only. Prior to examine the alignment of polymer macroscopically, it is import to mention here that maximum absorption occurs along the polymer chains and minimum perpendicular to polymer chain for plane polarized light due maximum distribution of charge along the polymer chains [21]. Therefore; we have used this property to investigate the alignment of chain in presence of polarised light. In order to investigate the polymer alignment macroscopically, films were subjected to the measurement of polarized electronic absorption spectrum in the range 350 to 750 nm.

Fig. 6 (c) exhibits the polarized electronic absorption spectra of the pristine and 2D nano-hybrid films prepared by FTM. It can be seen that both of the parallel oriented thin films exhibits clear peaks around 537 nm and vibronic shoulder around 580 nm. However, there are clear differences observed in electronic absorption spectra for perpendicularly oriented films having nearly the same absorption intensity. Perpendicular oriented pristine PQT film exhibits shoulder peak almost at the same position as in parallel orientation. In order to investigate the optical anisotropy (alignment of the polymer) in these films, we have calculated the optical DR for both of the films, which was found to be 3.7 and 2.0 for composite hybrid and pristine PQT films, respectively. The enhancement in DR clearly indicates the two times enhancement in the optical anisotropy by GO nanosheets as compared to pristine PQT. It

is important to mention here that polymer chains absorb maximum light along the polymer backbone and minimum perpendicular to back bone. Therefore, DR is directly related to the polymer alignment in the film at macroscopic level. Here, our objective was to show the effect of 2D nanosheets on electronic absorption spectra and charge carrier transport in the composite system. It can be clearly seen that presence of 2D nanosheets results in to the enhancement of DR by two folds as compared to that pristine PQT. It has been observed here that \parallel -polarization light absorption spectrum of monohybrid film shows the red shift with well-resolved vibration band at higher wavelength, which is indication of interaction of light only with well-ordered parallel polymer chains. However, the \perp -polarization of light spectrum shows blue shift along with decreased resolution of vibration band on right shoulder. The blue shifting of absorption peak for \perp -polarization of light arises due to the interaction of light with non-stacked and disordered polymeric chains of PQT.

3.6. Electrical Characterization

In order to analyse the effect of 2D nanosheets and polymer alignment, mobility (μ) of film along and across (\parallel and \perp) to the direction of orientation and deduce the electronic parameters, oriented films of PQT were transferred on CYTOP coated SiO₂/Si(p) substrates (capacitance of 8 nF/cm²) from liquid substrate by stamping as shown in the Fig 1. Prior to deposition of gold (Au) electrode, the deposited film was washed with isopropanol, followed by drying in air for 15 min to remove any residual solvent. Later, nickel shadow mask was employed to deposit the source and drain electrodes at 10⁻⁶ Torr having the channel length (L) and width (W) of 20 μ m and 2 mm, respectively. All of the electrical characterizations were carried out under dark at 10⁻³ Torr using Keithley-2612 source measure unit. μ and other electrical parameters were extracted in the saturation region using equation-1 and 2 [33-34].

$$I_{ds} = \frac{W}{2L} \mu C_i (V_{gs} - V_{th})^2 \text{ ----- (1)}$$

$$\sigma = \frac{LI_{ds}}{WVd} \text{-----}(2)$$

μ of PQT was estimated for OFETs fabricated after depositing the channel with respected to \parallel (μ_{\parallel}) and \perp (μ_{\perp}) with respect to the orientation directions.

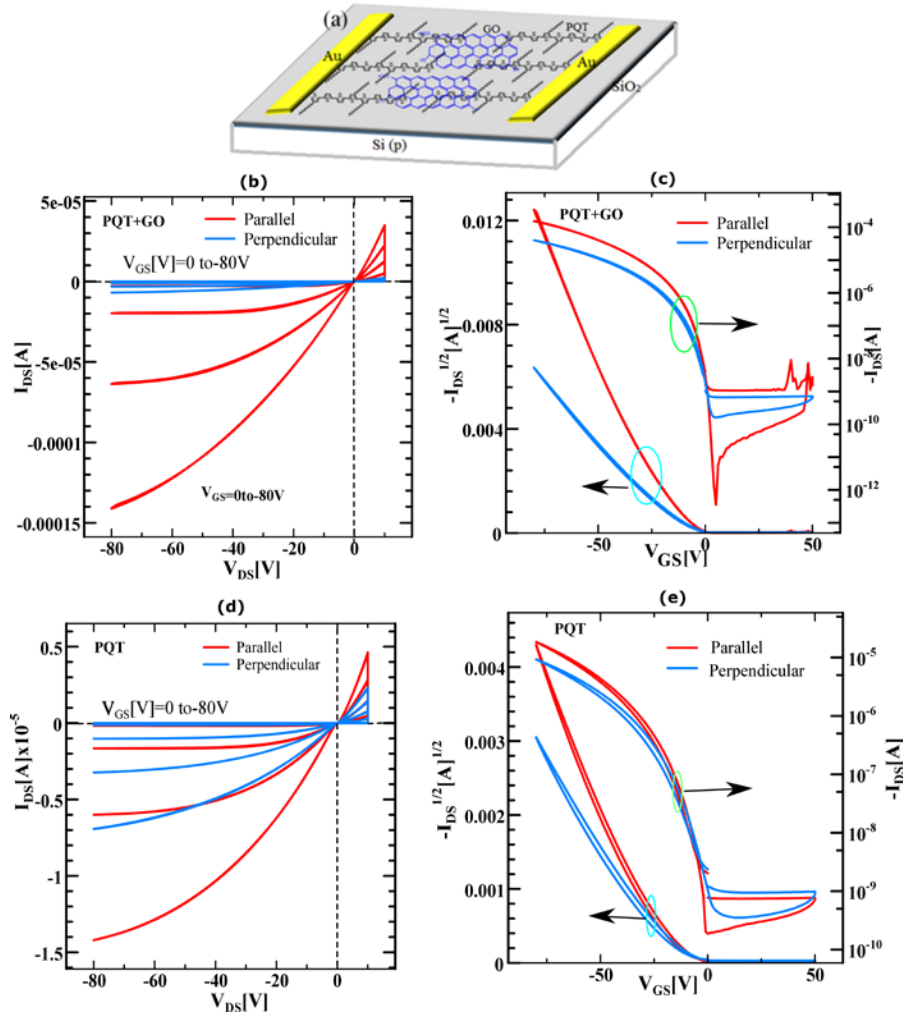


Fig. 7 (a) Schematic representation of PQT-GO OFET device structure used in this work. (b-c) output and transfer curve of nano-hybrid film of PQT/GO and (d-e) pristine PQT film based OFETs.

Obtained results from I-V measurements are shown in the Fig. 7(b-e) for the nano-hybrid and pristine polymer based OFETs. A perusal of this figure reveals typical p-type I_d-V_d output and I_d-V_g transfer characteristics in both of the cases. In order to calculate the μ , on/ off ratio and threshold voltage (V_{th}),

the saturated regime of transfer characteristics was chosen and extracted parameters are listed in the Table 1 along with the optical and electrical anisotropies.

Table 1. Electrical and Electronic parameters of the OFETs fabricated using oriented pristine PQT and its nano-hybrid thin films.

Electronic Parameter→ Devices↓		μ ($\text{cm}^2/\text{V.s}$)	On/off ratio	$\mu_{\parallel}/\mu_{\perp}$	A_{\parallel}/A_{\perp}	σ (S/cm)	
						$V_g=0\text{V}$	$V_g=80\text{V}$
PQT+GO	\parallel	0.11	10^6	4.2	3.7	1.02×10^{-6}	17.33×10^{-3}
	\perp	0.03	10^5			4.1×10^{-7}	3.07×10^{-3}
PQT	\parallel	0.02	10^5	2.2	2	4.2×10^{-7}	18.96×10^{-4}
	\perp	0.008	10^4			3.32×10^{-7}	10.69×10^{-4}

Using eq. 1, μ_{\parallel} of the oriented hybrid PQT/GO film was calculated and found to be $\sim 0.11 \text{ cm}^2/\text{V.s}$ with on/ off ratio 10^6 . However, the obtained value of maximum mobility for pristine polymer was $0.02 \text{ cm}^2/\text{V.s}$, which is nearly the same reported by Tripathi et.al [34]. Electrical anisotropies are following the same trends as compared to that of optical anisotropies for both the pristine PQT as well as nanocomposite films. Obtained charge carrier mobility for hybrid film is several folds more than that reported in the literature [34-37]. It is noteworthy that Tripathi et. al have reported DR ~ 22 with field effect mobility $0.02 \text{ cm}^2/\text{V.s}$. [34], however, in our case, we have got mobility of $0.11 \text{ cm}^2/\text{V.s}$ (DR=3.7), which is 5 fold higher. This enhancement in mobility can be justified considering the presence of GO nanosheets, which causes the formation of interconnected crystallites with enhanced polymer alignment and conjugation length. Further, the composite film shows electrical anisotropy of

4.2 and 6.2 fold higher mobility as compared to the pristine polymer along the polymer alignment direction. Thus, the achieved high mobility for composite film can be explained considering the promoted molecular self-assembly by 2D nanosheets of GO as evidenced by TEM, HR-TEM, STEM, GIXD and polarized electronic absorption spectral investigations. GO nanosheets are uniformly distributed and decorated with crystalline polymer nanostructure between two electrodes with highly edge on oriented and aligned PQT macromolecules. This high conductivity and mobility obtained in the composite film prepared by FTM can be explained via Mott's variable-range conduction mechanism, which state that there are multiple path for charge carrier transport in the hybrid materials. Percolation theory deals with a number of easy path for charge transport, present in a composite systems. The easy path in our hybrid system is self-assembled, crystalline, aligned and oriented polymer chains, which are interconnected via 2D GO sheets as depicted in Fig 7(a) and provides the easy path for charge percolation leading to facile charge transport.

A perusal of the Fig. 7 reveals that there was a positive shift in the V_{th} from -26 V for pristine PQT to -20 V for the PQT-GO nanohybrid based OFETs. This could be associated with enhancement of molecular ordering in the polymeric chains after incorporation of GO in PQT as evidenced by polarized absorption spectra shown in the Fig. 6 (c). A similar behaviour of positive shift in V_{th} upon introduction of Au nanoparticles in P3HT based OFETs has also been observed by Han et al, who advocated about the enhancement in the hole conduction due to increased crystallinity upon nanoparticle introduction up to certain optimal threshold limit [38]. In our case, TEM study reveals that GO nanosheets are uniformly distributed and decorated with crystalline CP nanostructures. Meanwhile, STEM, HR-TEM study reveals the formation of nano-fibril like structure having lamella of crystalline π - π stacking. However, comparative study of GIXD using HR-TEM images authorises the augmentation in crystallinity as well as highly edge on oriented film. Further, it has also been reported

that maximum mobility occurs along the polymer chains and in solution processable polymeric thin films they are either isolated or coupled via amorphous chain knotted between the domains [39]. Hybridization of PQT with GO nanosheets roots the creation of an unified domain either via GO or crystalline polymer. Therefore, the hybrid films having unified crystallites systems cause the charge carrier to delocalize over the long distances via domains. Thus, the decoration of GO with PQT contemporarily improves the crystallinity and facilitates the charge transport, which is responsible for the improvement in output current and mobility of the hybrid film. It is noteworthy to mention that polymer self-assembly causes change in work function and this change in work function leads to the change in the contact resistance. This might be another reason for the enhancement in mobility [40, 41]. Further, we have calculated the conductivity of films using equation 2 in \parallel and \perp oriented hybrid and pristine polymer film in OFET configuration at gate bias voltages of 0 V and 80 V in Ohmic region of I_{ds} - V_{ds} and results are listed in the table 1. It is obvious from results that conductivity is also depending upon the orientation of polymer chains. Maximum conductivity was observed in both case for \parallel configuration as listed in table 1, which is following same trends as field effect mobility.

In summary, we have successfully obtained the 4 layer thick GO nanosheets via ultra-sonication and implementation of phase transfer method for fabrication of PQT/GO nanohybrid thin films. Furthermore, these films fabricated by FTM are edge on oriented and exhibited optoelectrical anisotropy. Development of self-assembled, highly oriented, anisotropic nanocomposite film was confirmed by morphological characterization, electronic absorption and structural characterization. Finally, the electrical characterization in OFET configuration of composite thin films reveals the 2D nanosheets augmented optical and electrical anisotropy with field effect mobility of $0.11 \text{ V/cm}^2\text{s}$ and on/off ratio of 10^6 .

4. Conclusion

We have successfully obtained the GO nano sheets of 4- layers via ultra-sonication and phase transfer methods and characterized them by techniques like HR-TEM, XRD and Raman spectra prior to the fabrication of PQT decorated GO nanohybrid. Further, a high surface free energy liquid substrate based FTM technique was used as facile method for the fabrication of self-assembled, highly oriented, anisotropic and hybrid thin films of PQT decorated GO nanohybrid. The interrogation of as prepared film via morphological and structural investigations validates the fabrication of high quality self-assembled, edge-on oriented and homogenously distributed GO nanosheets in polymer films matrix. Further, investigation of alignment of CP/GO hybrid film at microscopic and macroscopic level via FFT and electronic absorption spectra, respectively, revealed the enhancement in alignment of polymer after incorporation of GO nanosheets. Finally, the charge transport were carried out in OFETs configuration and investigated in \parallel and \perp to the polymer alignment directions, which demonstrated the superior device performance with $0.11 \text{ cm}^2/\text{V.s}$ field effect mobility and 10^6 on/off ratio as compared to that of corresponding devices based on pristine PQT. This enhancement in charge transport upon molecular alignment has been confirmed by the evidences from morphological, structural, FFT, polarised electronic absorption spectral characterizations. Thus, our study has elucidated a path to use liquid air interface to obtain a self-assembled, highly oriented, anisotropic nano hybrid thin films towards the successful application in the area of organic electronics.

Acknowledgements

Authors are thankful to Dr. A K Mishra (SMST, IIT BHU), CIF, IIT (BHU) Varanasi for providing Raman and other characterization facilities.

Supporting Information- It Includes synthesis procedure of GO, real picture of phase transferred GO, AFM height image and XRD of as synthesised GO nanosheets.

References

1. C. Reese, M. Roberts, M.-M. Ling, and Z. Bao, Organic thin film transistors, *Mater. Today*, 7 (2004)20-27.
2. X. Guo, Y. Xu, S. Ogier, T. N. Ng, M. Caironi, A. Perinot, L. Li, J. Zhao, W. Tang, R. A. Sporea, A. Nejm, J. Carrabina, P. Cain, and F. Yan, Current Status and Opportunities of Organic thin film transistors Technologies, *IEEE Trans. Electron Devices*, 64, (2017) 1906-1921.
3. S. R. Forest, The path to ubiquitous and low cost organic electronic appliances on plastic, *Nature*, 428 (2004) 911-918.
4. H. Klauk Organic thin film transistors, *Chem. Soc. Rev.*, 39 (2010)2643-2666.
5. M. Eslamian, Inorganic and organic solution Processed thin film devices, *Nano-Micro Lett.* 9 (2017)1-23.
6. J. Shin, T. R. Hong, T. W. Lee, A. Kim, Y. H. Kim, M. J. Cho, D. H. Choi, Template-Guided Solution-Shearing Method for Enhanced Charge Carrier Mobility in Diketopyrrolopyrrole-Based Polymer Field-Effect Transistors, *Adv. Mater.* 26, (2014) 6031-6035.,
7. Y. Diao, B. C-K. Tee, G. Giri, J. Xu, D. H. Kim, H. A. Becerril, R. M. Stoltenberg, T. H. Lee, G. Xue, S. C. B. Mannsfeld, Z. Bao, Solution coating of large-area organic semiconductor thin films with aligned single-crystalline domains, *Nat. Mater.* 12 (2013)665-671.

8. J.H. Li, Y. Xi, L. D. Pozzo, J. T. Xu, C. K. Luscombe, Macroscopically aligned nanowire arrays of π -conjugated polymers via shear-enhanced crystallization, *J. Mater. Chem. C* 5 (2017) 5128-5134.
9. J.-M. Verilhac, R. Pokrop, G. LeBlevenec, I. Kulszewicz-Bajer, K. Buga, M. Zagorska, S. Sadki, and A. Pron, Molecular Weight Dependent Charge Carrier Mobility in Poly(3,3'-dioctyl-2,2':5',2'-terthiophene), *J. Phys. Chem. B*, 110 (2006)13305-13309.
10. R. Ahmad, R. Srivastava, S. Yadav, S. Chand, and S. Sapra, Functionalized 2D-MoS₂-Incorporated Polymer Ternary Solar Cells: Role of Nanosheet-Induced Long-Range Ordering of Polymer Chains on Charge Transport, *ACS Appl. Mater. Interfaces* 9 (2017)34111-34121.
11. D. Chaudhary, S. Munjal, N Khare , V.D. Vankar, Bipolar resistive switching and nonvolatile memory effect in poly (3-hexylthiophene)-carbon nanotube composite films, *Carbon*, 130 (2018) 553-558.
12. E. Istif, J. Herna´ndez-Ferrer, E. P. Urriolabeitia, A. Stergiou, N. Tagmatarchis, G. Fratta, M. J. Large, A. B. Dalton, A. M. Benito and W. K. Maser, Conjugated Polymer Nanoparticle-Graphene Oxide Charge-Transfer Complexes, *Adv. Funct. Mater.*, 28 (2018)1707548(1-10).
13. J. R. Potts, D. R. Dreyer, C. W. Bielawski, R. S. Ruoff, Graphene based polymer nanocomposites, *Polymer* 52 (2011)5-25.
14. T. Ahn and H. Lee, Effect of annealing of polythiophene derivative for polymer light emitting diodes, *Appl. Phys. Lett.* 80 (2002) 392(1-3) .
15. T. J. Savenije, J. E. Kroeze, X. Yang, J. Loose, The effect of thermal treatment on the morphology and charge carrier dynamics in polythiophene- fullerene bulk heterojunction, *Adv. Funct. Matter*,15 (2005)1260-1266

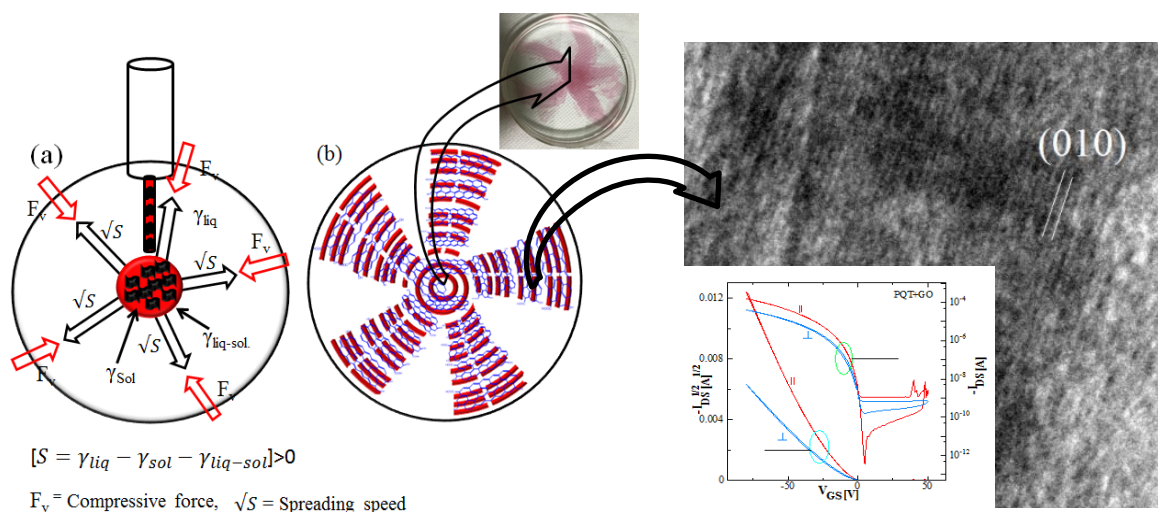
16. R. K. Pandey, A. K. Singh, C. Upadhyay, R. Prakash, Molecular self ordering and charge transport in layer by layer deposited poly (3, 3''-dialkylquaterthiophene) films formed by Langmuir-Schaefer technique *J. Appl. Phys.* 116, (2014)034311(1-9).
17. A. K. Geim, K. S. Novoselov, The rise of graphene, *Nature Mater.* **6**,(2007)183-191.
18. C. Soldano, A. Mahmood, E. Dujardin, Production, properties and potential of graphene, *Carbon*, 48 (2010) 2127-2150,
19. S. H. Bae, Y. Lee, B. K. Sharma, H. J. Lee, J. H. Kim, J. H. Ahn, Graphene-based transparent strain sensor, *Carbon* 51 (2013)236-241
20. A. Liscio, G. P. Veronese, E. Treossi, F. Suriano, F. Rossella, V. Bellani, R. Rizzoli, P. Samori, V. Palermo, Charge transport in graphene–polythiophene blends as studied by Kelvin Probe Force Microscopy and transistor characterization, *J. Mater. Chem.* **21**, (2011)2924-2931.
21. M. K. Singh, R. K. Pandey, R. Prakash . High-performance photo detectors based on hydrothermally grown SnO₂ nanostructure/r-GO hybrid materials, *Organ. Electron.* 50, (2017)359-366.
22. R. K. Pandey, W. Takashima, S. Nagamatsu, A. Dauendorffer, K. Kaneto, and R. Prakash, Macroscopic self ordering of solution processible poly (3, 3 ''-dialkylquaterthiophene) by floating film transfer method *J. Appl. Phys.* 114(2013) 054309(1-8).
23. J. Noh, S. Jeong, J.-Y. Lee, Ultrafast formation of air-processable and high-quality polymer films on an aqueous substrate, *Nat. Comm* 2016, DOI: 10.1038/ncomms12374.
24. A. Bellunato, H. A. Tash, Y. Cesa, and G. F. Schneider, Chemistry at the Edge of Graphene, *Chem. Phys. Chem.* 17, (2016)785 – 801
25. A. D. Dussaud, and S. M. Troian, Dynamics of spontaneous spreading with evaporation on a deep fluid layer, *Phys. Fluids* 10 (**1998**) 23–38.

26. A. H. Demond, and A. S. Lindner, Estimation of interfacial tension between organic liquids and water, *Sci. Technol.* 27 (1993) 2318–2331.
27. M. Pandey, S. S. Pandey, S. Nagamatsu, S. Hayase, W. Takashima, Controlling Factors for Orientation of Conjugated Polymer Films in Dynamic Floating-Film Transfer Method, *J. Nanosci. Nanotechnol.* 17 (2017)1915-1922.
28. M. Pandey, S. Sadakata, S. Nagamatsu, S. S. Pandey, S. Hayase, W. Takashima, Layer-by-layer coating of oriented conjugated polymer film towards anisotropic electronics, *Synth. Met.* 227, (2017)29-36.
29. J. Soeda, H. Matsui, T. Okamoto, I. Osaka, K. Takimiya, J. Takeya, Highly oriented polymer semiconductor films compressed at the surface of ionic liquids for high-performance polymeric organic field-effect transistors *Adv. Mater* 26 (2014) 6430(1-5).
30. M. Brinkman, L. Harmann, L. Biniek, K. Tremel, N. Kayunkid, Orienting semi-conducting π -conjugated polymers, *Macromol. Rapid Commun.* 35 (2014)9-26.
31. Y.-J. Kim, H.-T. Jung, C. W. Ahn, and H.-J. Jeon, Simultaneously Induced Self - Assembly of Poly(3 - hexylthiophene) (P3HT) Nanowires and Thin - Film Fabrication via Solution - Floating Method on a Water Substrate, *Adv. Mater. Interfaces* 2017, 1700342, DOI: 10.1002/admi.201700342.
32. L. Biniek, S. Pouget, D. Djurado, E. Gonthier, K. Tremel, N. Kayunkid, E. Zaborova, N. Crespo-Monteiro, O. Boyron, N. Leclerc, High-Temperature Rubbing: A Versatile Method to Align π -Conjugated Polymers without Alignment Substrate, *Macromolecules* 47 (2014) 3871-3879.

33. J. Sun, B.-J. Jung, T. Lee, L. Berger, J. Huang, Y. Liu, D. H. Reich, and H. E. Katz, Tunability of Mobility and Conductivity over Large Ranges in Poly(3,3''-didodecylquaterthiophene)/Insulating Polymer Composites, *ACS Appl. Mater Interfaces*, 1 (2009) 412-419
34. A. S. M. Tripathi, M. Pandey, S. Sadakanta, S. Nagamatsu, W. Takashima, S. Hayase, S. S. Pandey, Anisotropic charge transport in highly oriented films of semiconducting polymer prepared by ribbon-shaped floating film, *Appl. Phys. Lett.* 112 (2018) 123301(1-4).
35. C. Kumar, G. Rawat, H. Kumar, Y. Kumar, R. Prakash, S. Jit, Electrical and ammonia gas sensing properties of poly (3, 3''-dialkylquaterthiophene) based organic thin film transistors fabricated by floating-film transfer method, *Organ. Electron.* 48 (2017) 53-60.
36. B. S. Ong, Y. Wu, P. Liu, S. Gardner, Structurally Ordered Polythiophene Nanoparticles for High-Performance Organic Thin-Film Transistors, *Adv. Mater.* 17 (2005)1141-1144.
37. T. Kushida, T. Nagase, H. Naito, Angular distribution of field-effect mobility in oriented poly[5,5'-bis(3-dodecyl-2-thienyl)-2,2'-bithiophene] fabricated by roll-transfer printing, *Appl. Phys. Lett.* 104 (2014)93304(1-3).
38. S-T. Han, Y. Zhou, Z-X. Xu and V. A. L. Controllable threshold voltage shifts of polymer transistors and inverters by utilizing gold nanoparticles; *Appl. Phys. Lett.* 101, 033306 (2012)
39. N. Kleinhenz, M. A. McBride, N. Persson, D. Choi, Z. Xue, P. H. Chu, M. A. Grover, G. Wang, E. Reichmanis, and Z. Yuan, Ordering of Poly(3-hexylthiophene) in Solutions and Films: Effects of Fiber Length and Grain Boundaries on Anisotropy and Mobility, *Chem. Mater.*, 28 (2016)3905-3913.

40. M. Baghgar, M. D. Barnes, Work Function Modification in P3HT H/J Aggregate Nanostructures Revealed by Kelvin Probe Force Microscopy and Photoluminescence Imaging; ACS Nano, , **9**(2015) 7105-7112.
41. K. Bhargava, M. Shukla and V. Singh; Comparative analysis of contact resistance and photoresponse in poly(3-hexylthiophene) and poly(3-octylthiophene) based organic field-effect transistors, Synthetic Metals, 233, (2017) 15-21.

Graphical Abstract



(a) Surficial flow of hybrid solution on the liquid substrate depends on spreading coefficient S which is directly connected $S = \gamma_{liq} - \gamma_{sol} - \gamma_{liq-sol}$. (b) Positive S results in a surficial flow of solution. However viscous force (F_v) act as compressive force, results in formation of uniform compact, aligned and oriented hybrid thin film in star shape. HR-TEM and transfer curve depicts the GO induced alignment, orientation of polymer chain and high mobility hybrid film.

*Note- R. K. Pandey and A. S. M. Tripathi have contributed equally.